



*Supplement of*

## **Causal influences of El Niño–Southern Oscillation on global dust activities**

**Thanh Le and Deg-Hyo Bae**

*Correspondence to:* Deg-Hyo Bae (dhbae@sejong.ac.kr) and Thanh Le (levinhthanh.lvt@gmail.com)

The copyright of individual parts of the supplement might differ from the article licence.

## 1 **Text S1**

2 The ENSO index was computed as the average sea surface temperature (SST) anomalies in the  
3 Niño 3.4 area (120–170°W; 5°N–5°S) in boreal winter (December–January–February, DJF).  
4 Confounding factors (i.e., the dipole mode index (DMI; Saji et al., 1999), the Southern Annular  
5 Mode (SAM) and the North Atlantic Oscillation (NAO; e.g., Hurrell et al., 2003)) may have  
6 effects on the connections between ENSO and dust deposition. The DMI was given as the  
7 difference in boreal fall (September–October–November, SON) SST anomalies between two  
8 Indian Ocean regions of the western pole (50–70°E; 10°N–10°S) and southeastern pole (90–  
9 110°E; 0°N–10°S). The SAM (Cai et al., 2011) was calculated as the first empirical orthogonal  
10 function (EOF) of the boreal summer (June–July–August, JJA) sea level pressure (SLP)  
11 anomalies for the region of 40–70°S. The NAO index is computed as the EOF of boreal winter  
12 (DJF) SLP anomalies in the North Atlantic area (90°W–40°E, 20°–70°N).

13 We estimate the probability of no Granger causality by applying a test of Granger causality (Le  
14 and Bae, 2020; Mosedale et al., 2006; Stern and Kaufmann, 2013) for the multivariate predictive  
15 model shown in equation 1. For computing the degree of uncertainty, we followed recent  
16 guidance (Stocker et al., 2013) and utilized the terms ‘very unlikely’, ‘unlikely’, ‘likely’ for the  
17 0–10%, 0–33%, and 66–100% probability of the likelihood of the outcome, respectively. For  
18 example, if the  $p$ -value is less than 0.33, the result indicates that ENSO is unlikely to display no  
19 Granger causality on dust deposition. In this instance, we conclude that ENSO has ‘causal effect’  
20 on dust deposition.

## 21 **References**

- 22 Cai, W., Sullivan, A. and Cowan, T.: Interactions of ENSO, the IOD, and the SAM in CMIP3  
23 Models, *J. Clim.*, 24(6), 1688–1704, doi:10.1175/2010JCLI3744.1, 2011.
- 24 Hurrell, J. W., Kushnir, Y., Ottersen, G. and Visbeck, M.: An overview of the North Atlantic  
25 Oscillation, in *Geophysical Monograph American Geophysical Union*, pp. 1–35, American  
26 Geophysical Union., 2003.
- 27 Le, T. and Bae, D.-H.: Response of global evaporation to major climate modes in historical and  
28 future Coupled Model Intercomparison Project Phase 5 simulations, *Hydrol. Earth Syst. Sci.*,  
29 24(3), 1131–1143, doi:10.5194/hess-24-1131-2020, 2020.
- 30 Mosedale, T. J., Stephenson, D. B., Collins, M. and Mills, T. C.: Granger Causality of Coupled  
31 Climate Processes: Ocean Feedback on the North Atlantic Oscillation, *J. Clim.*, 19(7), 1182–

- 32 1194, doi:10.1175/JCLI3653.1, 2006.
- 33 Saji, N. H., Goswami, B. N., Vinayachandran, P. N. and Yamagata, T.: A dipole mode in the  
34 tropical Indian Ocean, *Nature*, 401(6751), 360–363, doi:10.1038/43854, 1999.
- 35 Stern, D. I. and Kaufmann, R. K.: Anthropogenic and natural causes of climate change, *Clim.*  
36 *Change*, 122(1–2), 257–269, doi:10.1007/s10584-013-1007-x, 2013.
- 37 Stocker, T. F., Qin, D., Plattner, G.-K., Alexander, L. V., Allen, S. K., Bindoff, N. L., Bréon, F.-  
38 M., Church, J. A., Cubasch, U., Emori, S., Forster, P., Friedlingstein, P., Gillett, N., Gregory, J.  
39 M., Hartmann, D. L., Jansen, E., Kirtman, B., Knutti, R., Kumar, K. K., Lemke, P., Marotzke, J.,  
40 Masson-Delmotte, V. Meehl, G. A., Mikhov, I. I., Piao, S., Ramaswamy, V., Randall, D., Rhein,  
41 M., Rojas, M., Sabine, C., Shindell, D., Talley, L. D., Vaughan, D. G. and Xie, S.-P.: Technical  
42 Summary, in *Climate Change 2013 - The Physical Science Basis*, edited by Intergovernmental  
43 Panel on Climate Change, pp. 31–116, Cambridge University Press, Cambridge., 2013.
- 44

45 **Table S1.** List of CMIP6 models used in this study.

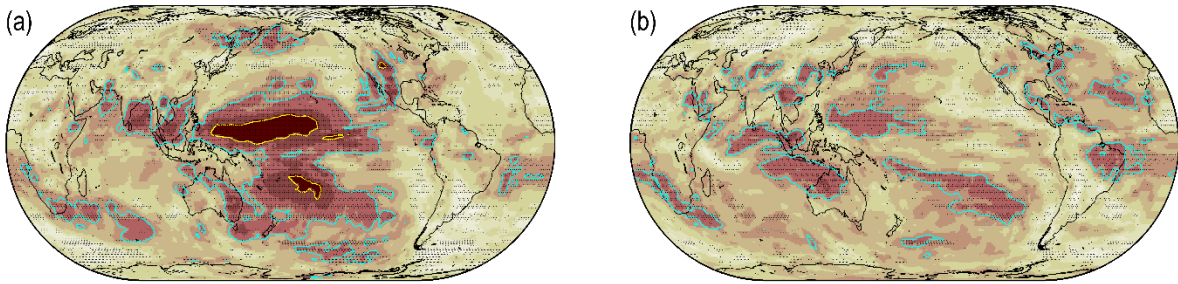
No.	Model name	Modelling center, country	Aerosol model	Atmospheric Chemistry model
1	CanESM5	CCCma, Canada	Interactive	Specified oxidants for aerosols
2	CESM2	NCAR, United States	MAM4	MAM4
3	CESM2_FV2	NCAR, United States	MAM4	MAM4
4	CESM2_WACCM	NCAR, United States	MAM4	MAM4
5	CESM2_WACCM_FV2	NCAR, United States	MAM4	MAM4
6	CNRM_ESM2_1	CNRM-CERFACS, France	TACTIC_v2	REPROBUS-C_v2
7	GFDL_ESM4	NOAA-GFDL, United States	Interactive	GFDL-ATMCHEM4.1
8	INM-CM4-8	INM, Russia	INM-AER1	None
9	INM-CM5-0	INM, Russia	INM-AER1	None
10	MIROC-ES2L	MIROC Japan	SPRINTARS6.0	None
11	MIROC6	MIROC, Japan	SPRINTARS6.0	None
12	UKESM1_0_LL	MOHC NERC, United Kingdom	UKCA-GLOMAP-mode	UKCA-StratTrop

46 **Table S2.** List of CMIP6 models used in this study with available data denoted by a check mark (✓). The  
 47 data unavailable are denoted by a cross (×).

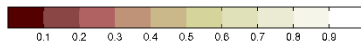
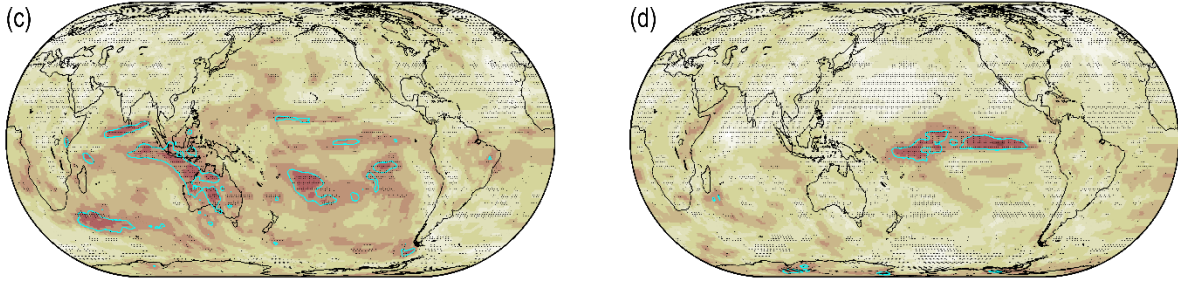
No.	Model name	Modelling center, country	dry dust	wet dust	od550dust	emidust
1	CanESM5	CCCma, Canada	✓	✓	✓	✓
2	CESM2	NCAR, United States	✓	✓	✓	✓
3	CESM2_FV2	NCAR, United States	✓	✓	✓	✓
4	CESM2_WACCM	NCAR, United States	✓	✓	✓	✓
5	CESM2_WACCM_FV2	NCAR, United States	✓	✓	✓	✓
6	CNRM_ESM2_1	CNRM-CERFACS, France	✓	✓	×	✓
7	GFDL_ESM4	NOAA-GFDL, United States	✓	✓	×	×
8	INM-CM4-8	INM, Russia	✓	✓	✓	✓
9	INM-CM5-0	INM, Russia	✓	✓	✓	✓
10	MIROC-ES2L	MIROC Japan	✓	✓	×	✓
11	MIROC6	MIROC, Japan	✓	✓	✓	✓
12	UKESM1_0_LL	MOHC NERC, United Kingdom	✓	✓	✓	✓

48

MODELS MEAN: ENSO - SPRING DRY DUST PERIOD 1850-2014 EXPERIMENT HISTORICAL      MODELS MEAN: ENSO - SUMMER DRY DUST PERIOD 1850-2014 EXPERIMENT HISTORICAL

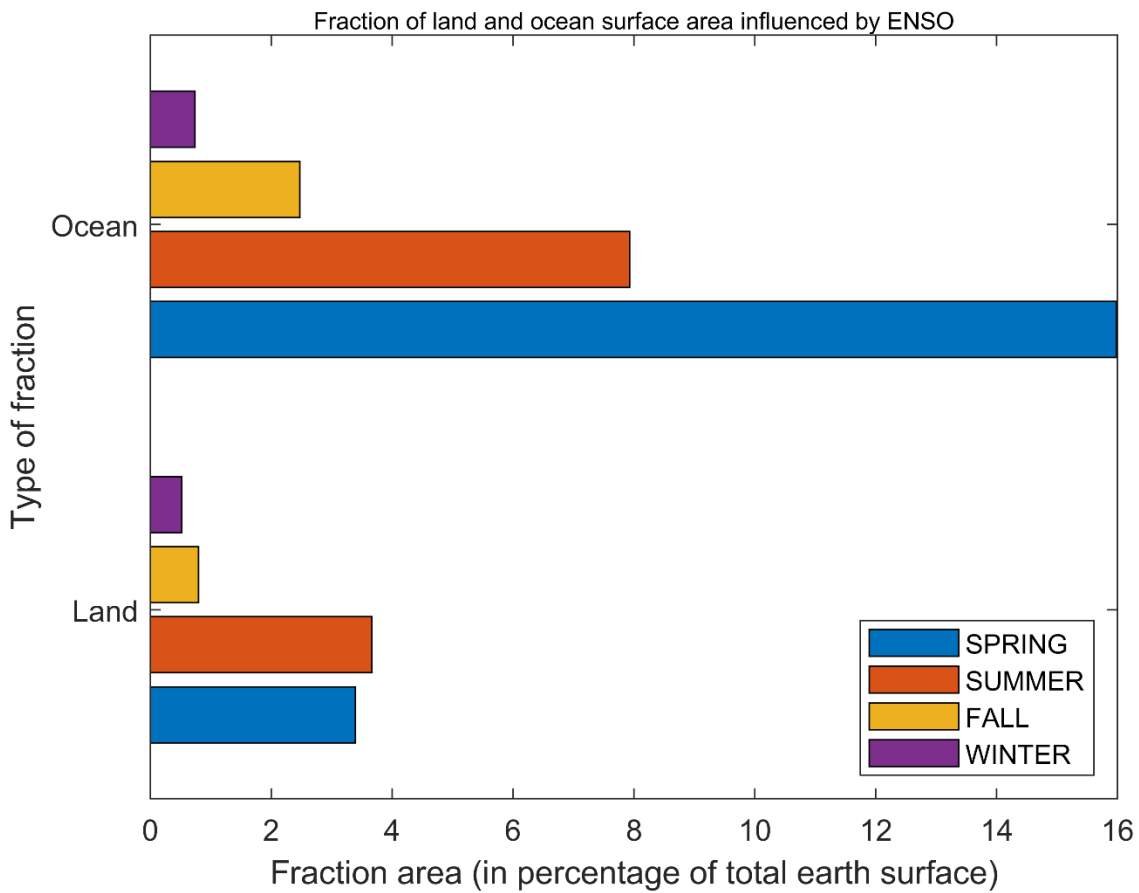


MODELS MEAN: ENSO - FALL DRY DUST PERIOD 1850-2014 EXPERIMENT HISTORICAL      MODELS MEAN: ENSO - WINTER DRY DUST PERIOD 1850-2014 EXPERIMENT HISTORICAL



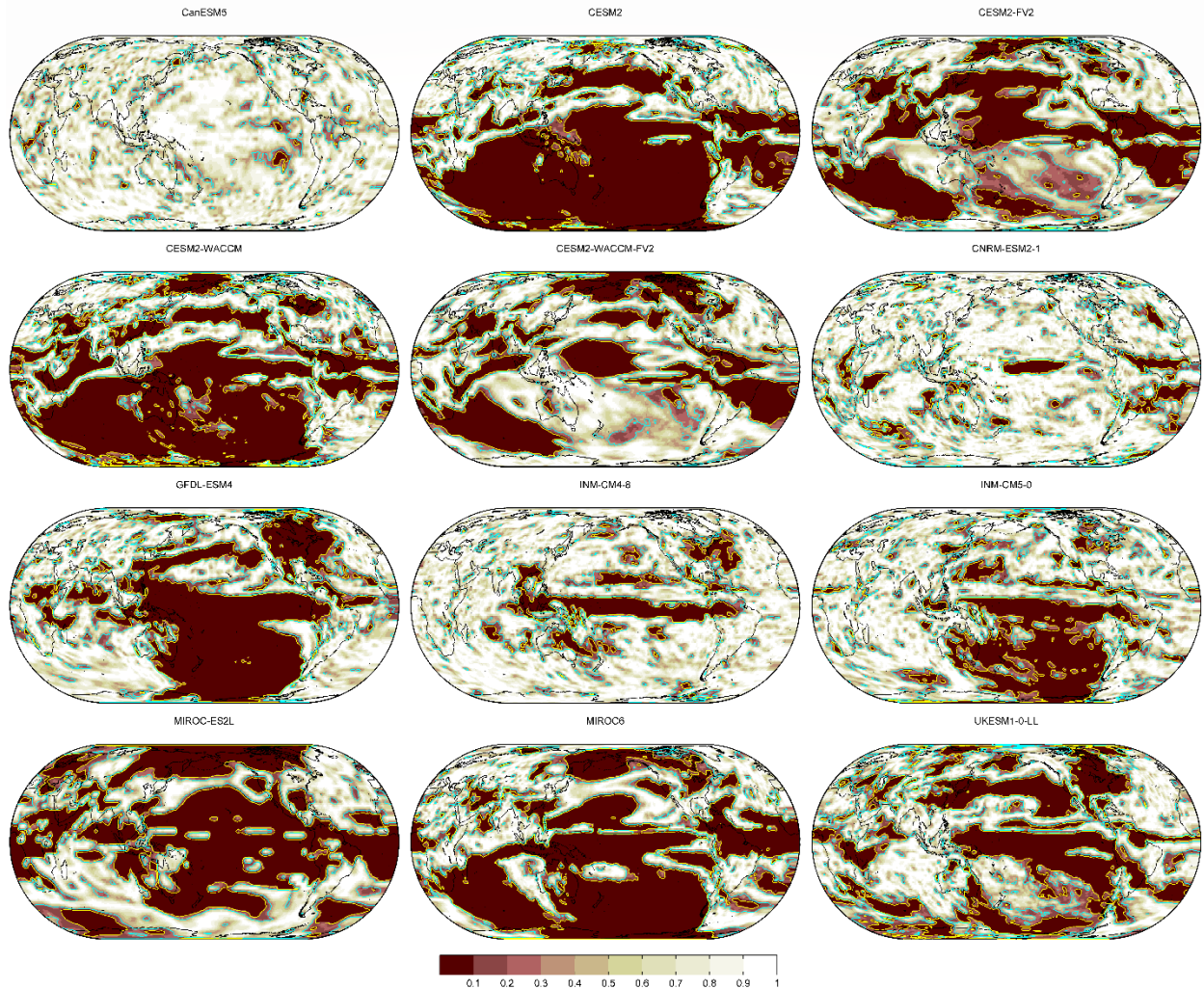
49

50 **Figure S1.** Multi-model mean probability map of no Granger causality from ENSO [DJF] to the  
51 following seasonal mean dry dust deposition over the period 1850-2014 of the historical simulation. (a)  
52 Spring [MAM]. (b) Summer [JJA]. (c) Fall [SON]. (d) Winter [DJF]. Stippling demonstrates that at least  
53 70% of total models show agreement on the mean probability of all models at a given grid point. The  
54 cyan and yellow contour lines signify  $p$ -value = 0.33 and 0.1, respectively. Brown shades denote a low  
55 probability for the absence of Granger causality. ENSO: El Niño–Southern Oscillation.



56

57 **Figure S2.** Fraction of total Earth-surface over land and ocean with probability for no Granger causality  
 58 from ENSO to seasonal mean dry dust deposition lower than 0.33 (i.e.,  $p$ -value < 0.33). Fraction areas  
 59 influenced by ENSO on Spring, Summer, Fall and Winter dry dust deposition are displayed in blue, red,  
 60 yellow, and purple bars, respectively. ENSO: El Niño–Southern Oscillation.



61

62 **Figure S3.** As in Figure 1, but for the probability of no Granger causality of ENSO on annual mean wet  
 63 dust deposition over the period 1850-2014 for the historical simulation of 12 individual models (see  
 64 Tables S1 and S2). ENSO: El Niño–Southern Oscillation.